Dynamics and stabilization of the Elettra storage-ring free-electron laser

G. De Ninno,[1] A. Antoniazzi,[2] B. Diviacco,[1] D. Fanelli,[2] L. Giannessi,[3] R. Meucci,[4] and M. Trovó[1]
[1]*Sincrotrone Trieste, 34012 Trieste, Italy*
[2]*Dipartimento di Energetica, Università di Firenze, INFN, 50139 Firenze, Italy*
[3]*ENEA, CP-65 00044 Frascati, Rome, Italy*
[4]*INOA, 50125 Florence, Italy*
(Received 11 December 2004; published 30 June 2005)

The ultimate performance of a storage-ring free-electron laser in terms of light stability and extracted power depends on the possibility of simultaneously controlling the electron-beam and laser dynamics. As a preliminary requirement, the level of longitudinal and transverse electron-beam stability must be high enough to guarantee the laser start-up and growth. This is usually obtained by means of dedicated feedback systems. Once such a requirement is satisfied, the possibility of establishing and maintaining a continuous-wave operation mode finally resides in a deep understanding of the strongly coupled laser-electrons dynamics. For this purpose, we have developed a simple theoretical model which has been proved to be able to provide insight into the evolution of the laser intensity. In this framework, we have also proposed the possibility of utilizing a derivative closed-loop feedback to create or enlarge the region of stable signal. A feedback of this type has been implemented on the Elettra storage-ring free-electron laser. The obtained results, which fully confirm our predictions, are discussed in this paper.

DOI: 10.1103/PhysRevE.71.066504 PACS number(s): 41.60.Cr, 05.45.−a, 29.20.Dh

I. INTRODUCTION

Instabilities of different nature may affect the dynamics of electron beams circulating in a storage ring (SR) [1,2], and cause severe limitation in the performance of devices dedicated to exploitation of synchrotron radiation or to free-electron laser (FEL) operation. The origin of such instabilities can be traced back either to the electromagnetic wake field which, generated by the interaction between the electron beam and its environment (e.g., vacuum pipe, low-gap chambers, discontinuities, etc.), reacts on electrons disturbing their motion, or to external perturbations (e.g., line-induced modulations, mechanical vibrations, etc.).

When the current circulating into the ring is distributed in a few bunches, and the wake field induced by a given bunch is strong and persistent enough to act on the successive ones, a coherent oscillation of the beam dimensions (at frequencies of the order of tens of kilohertz) may develop (see, e.g., Ref. [3]). In this case, the beam can be stabilized by means of a feedback system which treats each bunch as an independent oscillator and applies a correcting kick through a dedicated magnet [4]. In other cases, the effect of the wake field is less "dramatic" and simply manifests in a smooth increase of the beam dimensions with the current circulating into the ring [1]. As for external perturbations, the induced instabilities are generally characterized by low frequencies (tens to a few hundred hertz) and may manifest in different ways, e.g., as a kick or as a continuous modulations [5]. The origin of these perturbations is often difficult to determine and, as a consequence, remedies are difficult to find.

In the case of the Elettra storage ring, both a multibunch and a local orbit feedback [4,6,7] are currently implemented. The role of the latter is to apply a closed bump compensation (at a given location of the storage ring) of the slow orbit drifts and low-frequency components affecting the transverse electron-beam dynamics. The combined action of the two systems is strengthened by the relatively high energy (2−2.4 GeV) at which the storage ring is normally operated: the higher the energy the more effective are the "natural" instabilities damping mechanisms due to synchrotron emission. This is generally enough to guarantee a satisfactory electron-beam (and, thus, light-source) stability for most users' experiment [8]. However, as will be made clear in the following, such a good level of stability is not sufficient to assure a stable and reproducible operation of the Elettra SRFEL.

In a SRFEL (whose schematic layout is shown in Fig. 1), the light emitted by electrons when passing through the (static and periodic) magnetic field generated by an optical klystron1 [30] is stored in an optical cavity and amplified during successive interactions with the electron beam. The amplification is obtained to the detriment of the electron-beam energy, whose spread increases with the growth of the intracavity power. The heating of the electron bunch due to the laser onset leads to the reduction of the amplification gain until the latter reaches the level of the cavity losses (laser saturation). The electron-beam energy is recovered, turn-by-turn, by means of a device, called radio frequency (see Fig. 1), which supplies to electrons the energy they lose due to synchrotron and FEL radiation. Such a device also allows slight modification of the beam revolution period.

Since it originates from the synchrotron radiation, the laser temporal structure is naturally characterized by a train of micropulses (whose duration is of the order of tens of picoseconds) separated by the interbunch temporal distance (hundred of nanoseconds). On a larger (millisecond) temporal scale, the FEL dynamics depends strongly on the longitudinal overlap between the electron bunch(es) and the laser pulses at each pass inside the interaction region. A given temporal detuning, i.e., a difference between the electron-beam revolution period and the photon's round trip inside the

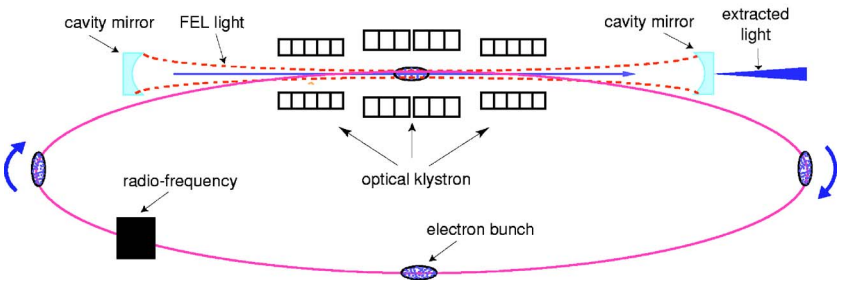

FIG. 1. Schematic layout of a storage-ring free-electron laser.

optical cavity, leads to a cumulative delay between the electrons and the laser pulses. The laser-electron detuning can be experimentally controlled either modifying the electron-beam revolution period (through a variation of the radio-frequency phase) or by changing the distance between the mirrors of the optical cavity. Due to a better sensitivity, the former method is generally preferred. In the ideal conditions, i.e., with a perfectly stable electron beam, the laser intensity may then appear "continuous wave" ("cw") for a weak or strong detuning, or show a pulsed behavior for an intermediate detuning amount [10,11]. The central cw zone of the detuning curve is interesting for user applications: in this zone, the laser is indeed characterized by a regular train of micropulses and by the maximum average power; moreover, the signal is the closest to the Fourier limit [12]. However, the "ideal" behavior, namely the existence of a stable regime around the perfect tuning, is difficult to obtain. The reason for that is twofold. First, the natural extension of the central cw zone is generally very narrow: a detuning of a few femtoseconds is indeed enough for inducing a sharp transition to the pulsed behavior. Moreover, the laser evolution inside the optical cavity is particularly sensitive to any electron-beam instability.

If the electron beam is stable enough for the cw region to be observed, the perfect tuning condition can be maintained by means of dedicated feedback systems which periodically modify the beam revolution period to keep the laser-electron synchronism. This strategy, successfully adopted for the Super ACO and UVSOR SRFELs [13,14], cannot be implemented when, as in the case of Elettra, the electron-beam instabilities prevent the laser intensity from reaching the stable behavior, even close to the perfect synchronism [15]. In this respect, it is worth stressing that the increased sensitivity to beam instabilities showed by Elettra is mainly due to its higher gain and larger damping time (which also means higher "reactivity") with respect to SRFELs of previous generation.

The possibility of further improving the performance of a "high gain" SRFEL resides in a deeper understanding of the mechanisms through which the system may lose its stability. This includes both the natural transition to the pulsed regime when increasing the laser-electron temporal detuning, and the destabilization, which may combine with a concurrent detuning, due to external electron-beam perturbations. As for the former point, a careful study has been recently carried out [16,17], which allowed us to provide explicit expressions for the asymptotic values of the main statistical parameters of the laser distribution as a function of the detuning amount. Moreover, the transition between stable and unstable regimes has been characterized as a Hopf bifurcation. On the basis of these results, we suggested the use of a derivative closed-loop feedback to delay the bifurcation, hence enlarging the region of stable signal. Further numerical studies, which will be presented in this paper, showed that a derivative feedback is also effective in counteracting external instabilities. A feedback of this type has been implemented on the Elettra SRFEL and shown to be able to induce a (quasi)- cw behavior of the laser intensity. This is in excellent agreement with theoretical predictions. The paper is organized as follows. In Sec. II we report the characteristics of the Elettra SRFEL when operated in the "natural" regime. After having briefly recalled, in Sec. III, the theoretical framework which can be used to gain insight into the evolution of the system, in Sec. IV we show that the observed unstable behavior of the laser intensity can be reproduced numerically by means of suitable modulation on the laser-electron detuning. Then, we demonstrate the stabilizing effect of the derivative feedback. Finally, Sec. V is devoted to drawing conclusions and perspectives.

II. THE NATURAL REGIME OF THE ELETTRA SRFEL

Thanks to the combination of high-quality electron beam (i.e., low emittance, short bunch length) [18], adjustable undulator parameters [19], and robustness of the high-reflectivity mirrors of its optical cavity [20], the European SRFEL at Elettra can be operated in the large electron-beam energy range from 0.75 to 1.5 GeV (the latter being the highest energy used so far for a SRFEL). This flexibility allowed extension of the accessible spectral range down to the VUV [21] and improvement of the FEL compatibility with other synchrotron radiation users interested in a few bunching filling of the storage ring [22].

However, as already mentioned, the quality of the electron-beam limits the source performance. Figure 2 shows a comparison between the behavior of the macro-temporal laser intensity as a function of the laser-electron detuning for the Elettra and Super-ACO [23] SRFELs. In the case of Super ACO, the laser dynamics is not significantly affected by the electron-beam instabilities: the intensity curve shows three cw and two pulsed zones, depending on the detuning. The pulsed regime is characterized by a single natural frequency which lies between 300 and 400 Hz and whose exact value is a function of the detuning [24]. On the contrary, the

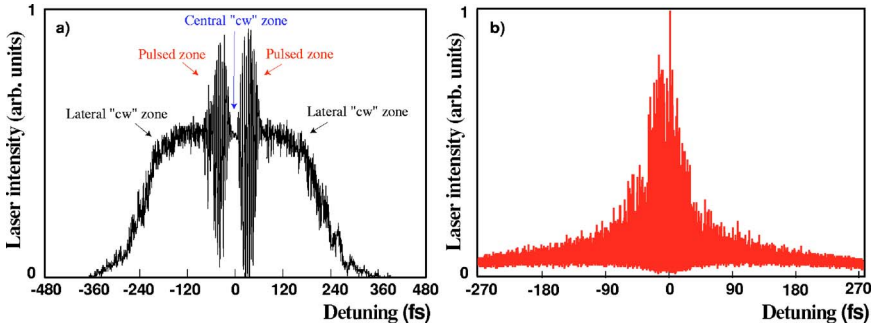

FIG. 2. Typical detuning curves (i.e., laser intensity as a function of detuning amount) obtained for the case of the Super-ACO (a) and Elettra (b) SRFELs.

Elettra laser intensity is irregularly pulsed over the whole detuning region. A typical example of such irregular behavior is shown in Fig. 3(a). The analysis of the spectrum, shown in Fig. 3(b), brings into evidence the strong influence of electron-beam instabilities on the laser dynamics. The noisy behavior is characterized by four strong harmonics. The two peaks at 300 and 350 Hz are probably induced by the natural laser response to detuning, as in the case of Super ACO. The fact that two different frequencies are observed may reflect a variation of the detuning during the period of signal acquisition (i.e., 100 ms). This scenario is supported by the presence of the two peaks at at 50 and 100 Hz. This low-frequency perturbation is systematically observed and can be directly related to the dynamics of the electron beam. Figure 4(a) shows a streak camera image of the electron beam in absence of FEL oscillation. A regular modulation at 100 Hz is displayed. In fact, the oscillation of the electron-beam centroid position [see Fig. 4(b)] induces analogous oscillations of the laser-electron detuning. The resulting perturbation on the laser dynamics is generally strong enough to switch it off periodically, even close to the perfect synchronism. Sometimes, the laser intensity shows a more complex behavior, as displayed in Fig. 5. As will be shown in the next section, a modulation (of suitable amplitude and frequency) of the laser-electron detuning may be at the origin of the broadband spectrum of Fig. 5(b).

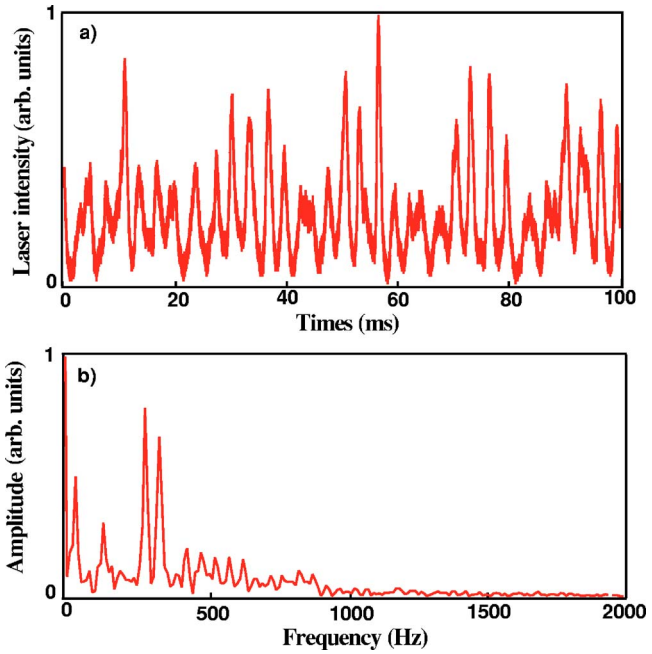

FIG. 3. (a) Typical temporal behavior of the Elettra FEL intensity close to the perfect laser-electron synchronism; (b) Fourier analysis of the signal shown in (a).

As already mentioned in the Introduction, a multibunch- and a local orbit feedback are currently used at Elettra for improving the electron-beam stability. When these systems are operational, a beneficial effect has been observed on both the transverse and longitudinal electron-beam dynamics [8]. However, we did not notice, at the same time, any significant benefits for the laser stability with respect to the operation without feedback. In fact, as will be made clear in the following, the level of electron-beam stability necessary to achieve a noticeable improvement of the laser signal is beyond the possibility of the feedback devices currently available. A new strategy to further increase the stability of the machine has been recently proposed, as a result of a deep theoretical investigation of the system dynamics. The study is based on the model that will be discussed in the next section.

III. THE MODEL

To model the longitudinal dynamics of the laser in the optical cavity, we use a system of three rate equations describing the coupled evolution of the electromagnetic field and the electron beam [25]. At each passage, the laser intensity profile, $I_n(\tau)$, is modified according to

$$I_{n+1}(\tau) = R^2 I_n(\tau - \epsilon)[1 + g_n(\tau)] + i_s(\tau), \tag{1}$$

where τ is the temporal position with respect to the centroid of the electron bunch distribution; $R(<1)$ is the reflectivity of the optical cavity mirrors; ϵ is the detuning parameter, i.e., the difference between the period of the photons inside the cavity and the electron revolution period (divided by the numbers of bunches); $i_s(\tau)$ accounts for the profile of the spontaneous emission of the optical klystron. The gain $g_n(\tau)$ is given by

$$g_n(\tau) = g_i \frac{\sigma_0}{\sigma_n} \exp\left[-\frac{\sigma_n^2 - \sigma_0^2}{2\sigma_0^2}\right] \exp\left[-\frac{\tau^2}{2\sigma_{\tau,n}}\right], \tag{2}$$

where g_i and σ_0 are the initial (laser-off) peak gain and beam energy spread; σ_n and $\sigma_{\tau,n}$ are the energy spread and bunch length after the nth interaction. The first exponential in the right-hand side of Eq. (2) accounts for the modulation rate of the optical-klystron spectrum, while the second one reproduces the temporal profile of the electron bunch distribution

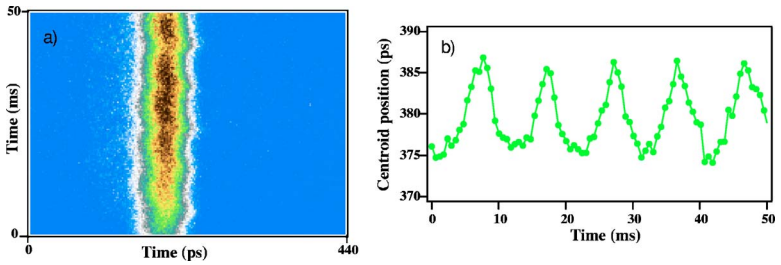

FIG. 4. (a) Streak camera image of the electron beam circulating in the Elettra storage ring (energy: 0.9 GeV, beam current: 0.5 mA). Along the vertical axis one can follow the evolution in time of the temporal beam distribution, while a horizontal cut provides the beam distribution profile. (b) Evolution of the position of the beam centroid as obtained by the analysis of (a).

(assumed to be Gaussian). The equation that governs the evolution of the laser-induced energy spread is

$$\sigma_{n+1}^2 = \sigma_n^2 + \frac{2\Delta T}{\tau_s}(\gamma I_n + \sigma_0^2 - \sigma_n^2), \tag{3}$$

where $\gamma=\sigma_e^2-\sigma_0^2$. Here, σ_e is the equilibrium value (i.e., that reached at the laser saturation) of the energy spread at the perfect tuning and $I_n=\int_{-\infty}^{\infty} I_n(\tau)d\tau$ is the laser intensity normalized to its equilibrium value (i.e., the saturation value for $\epsilon=0$); ΔT is the revolution period of the electrons in the ring (divided by the number of bunches); and τ_s is the synchrotron damping time.

Despite the simplicity, results obtained with this model show a remarkable agreement with experiments. In particular, a quantitative agreement has been found between the theoretical and the experimental detuning curve (see Fig. 2) for the case of Super ACO [24]. As pointed out in the previous section, the experimental detuning curve for Elettra does not present the central cw zone. In fact, using the parameters listed in Table I, the predicted width of the cw region is about 0.2 fs (±0.1 fs) around the perfect tuning.

This value is smaller than the finer tuning experimentally accessible to adjust the laser-electron synchronism. As a consequence, the stable regime is difficult to attain. Moreover, as will be shown in the following, a small perturbation of the detuning parameter (of the order of the width of the stable region) is enough for driving the system unstable even at the perfect tuning.

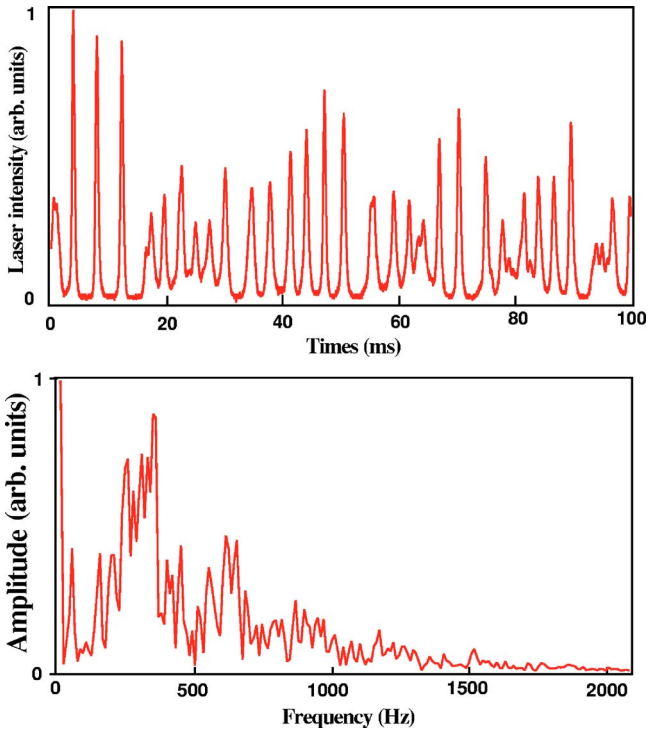

FIG. 5. (a) Typical temporal behavior of the Elettra FEL intensity close to the perfect laser-electron synchronism; (b) Fourier analysis of the signal shown in (a).

IV. STABILIZATION OF THE ELETTRA FEL

As already pointed out, the electron beam is subject to perturbations at low frequency (normally 50 and 100 Hz). This reflects in a modulation of the laser-electron detuning. In order to model this instability, we added the following equation to the system (1)–(3):

$$\epsilon_n = \epsilon_0 + A\sin(2\pi f \Delta T n), \tag{4}$$

where f is the frequency of the modulation, A its amplitude, and ϵ_0 its mean value. An equation of this type has been used to demonstrate that a SRFEL may be driven to deterministic chaos through a cascade of bifurcations [26,27].

Figure 6 shows numerical results assuming $f=50$ Hz and $\epsilon_0=0$ (oscillations around the perfect tuning) and different values of the amplitude A. The output signal is slightly modulated at the frequency f for values of A such that the system is maintained well inside the cw region. When A increases, the modulation amplitude increases. This happens until, for a given value of A close to the detuning threshold ($A\simeq 0.18$ fs in the case of the figure), there is a sharp tran-

TABLE I. Characteristics of the ELETTRA SRFEL for the numerical and experimental setting considered in this paper.

	Elettra
Beam energy (MeV)	900
τ_s (ms)	86
σ_0	1.12×10^{-3}
I (mA) (in four bunches)	15
σ_e/σ_0	$\simeq$1.3
Laser wavelength (nm)	250
g_i (%)	15
R (%)	$\simeq$96
ΔT (ns)	216
i_s	$\simeq4.3\times10^{-7}$

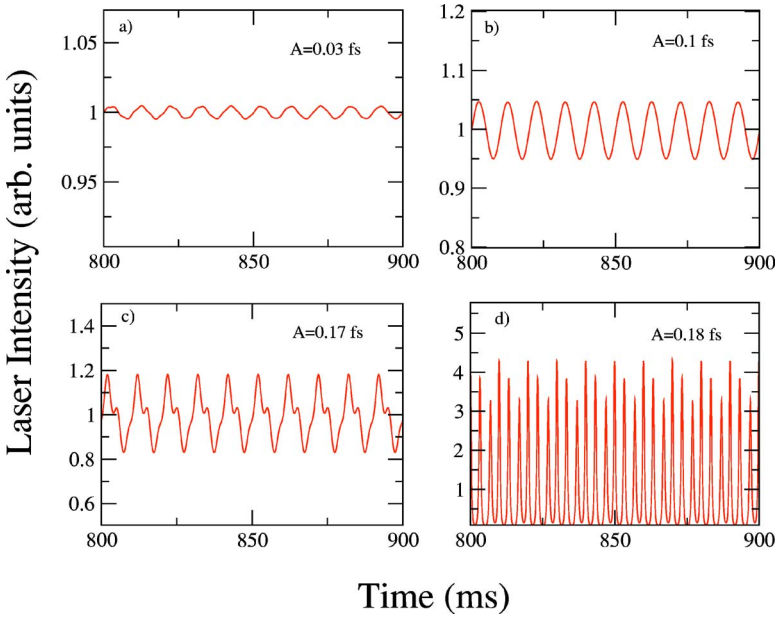

FIG. 6. Numerical results obtained with a modulation of the detuning parameter according to Eq. (4) with $f=50$, $\epsilon_0=0$, and different values of the amplitude A.

sition and the laser becomes pulsed. As anticipated, this shows that even a very small perturbation may destroy the continuous regime.

The modulation at 50 Hz of the laser-electron detuning allows us to reproduce qualitatively the observed laser intensity. This is for instance shown in Fig. 7, which refers to $\epsilon_0=0.05$ fs and $A=0.18$ fs. As in the experimental picture (see Fig. 3), the output signal is irregularly pulsed and the spectrum shows two peaks at 50 and 100 Hz as well as a double peak inside the natural response region. Note that in this case the modulation at 100 Hz is simply a harmonic of the one at 50 Hz. However, this is not always the case: sometimes the modulation at 100 Hz may manifest independently (see, e.g., Fig. 4) and/or in combination with the one at 50 Hz. Figure 8 shows the numerical result obtained when using a double-frequency modulation of the detuning

$$\epsilon_n = \epsilon_0 + A_1 \sin(2\pi f_1 \Delta T n) + A_2 \sin(2\pi f_2 \Delta T n), \qquad (5)$$

with $f_1=50$ Hz, $f_2=100$ Hz, and different sets of A_1 and A_2. The output signal and the spectral content are very close to the ones shown in Fig. 5.

In Ref. [16], a simplified formulation of system (1)–(3) was introduced and solved analytically. This allowed us to derive closed expressions for the main statistical parameters of the system (i.e., beam energy spread, intensity, centroid position, and rms value of the laser distribution) as a function of the detuning. Moreover, the transition between the "cw" and the pulsed regimes has been shown to be a Hopf bifurcation. This opened up the perspective of enlarging the stable region using a closed-loop derivative feedback [28]. The experimental procedure, sketched in Fig. 9, is as follows. A signal proportional to the FEL output power (produced, e.g., by the response of a photodiode) is sent to the stabilization system, made of a simple device to obtain the signal derivative, followed by an inverting amplifier with a variable gain. The obtained output is then used to modify the electron-beam revolution period (via the modification of the radio frequency), i.e., the value of the detuning ϵ. From a theoretical point of view, the detuning ϵ is replaced with the time-dependent quantity

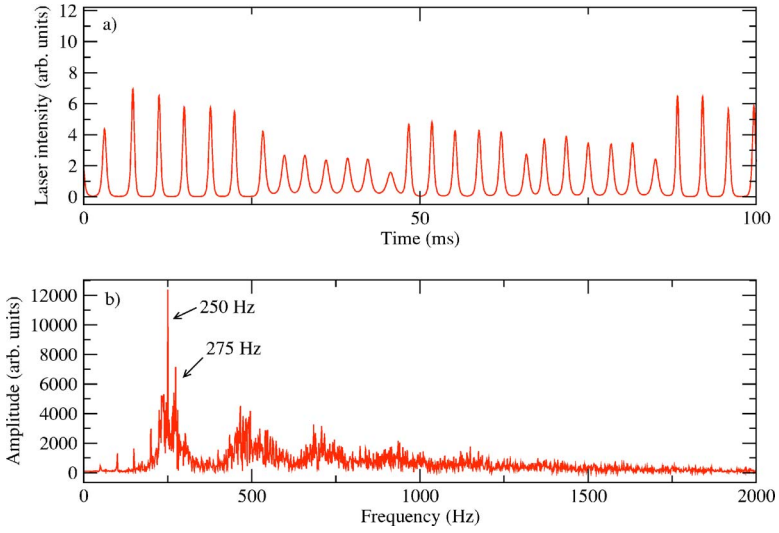

FIG. 7. Intensity and fast Fourier transform obtained combining Eqs. (1)–(4) with $\epsilon_0=0.05$ fs and $A=0.18$ fs. Numerical results to be compared with the experimental ones shown in Fig. 3.

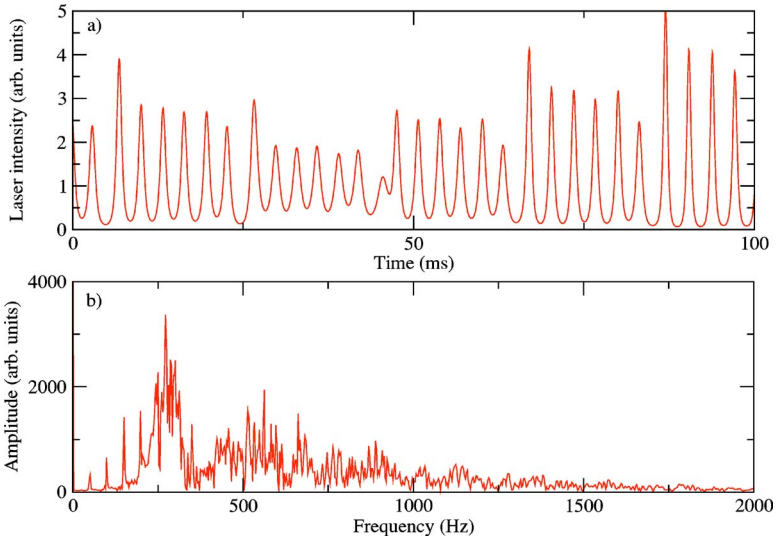

FIG. 8. Intensity obtained with a modulation of the detuning parameter according to Eq. (5). In this case $\epsilon_0=0.05$ fs, $A_1=0.14$ fs, and $A_2=0.1$ fs.

$$\epsilon_n = \hat{\epsilon}_0 + \beta(I_n - I_{n-1}), \tag{6}$$

where $\hat{\epsilon}_0$ is larger than the threshold value, ϵ_c, above which the system becomes unstable and $\beta \geqslant 0$. When the control is switched off, i.e., $\beta=0$, the laser is therefore unstable and displays periodic oscillations. For β larger than a certain threshold, β_c, the oscillations are damped and the laser behaves as if it was in the cw region. This procedure has been succesfully applied to extend the stable region of the Super-ACO FEL [29]. As will be immediately clear, the combination of Eqs. (4) and (6) gives a recipe for stabilizing the output signal of the Elettra FEL. In other words, we are going to show that the derivative feedback is effective also when, as in the case of Elettra, the cw region is "masked" by low-frequency instabilities perturbing the electron-beam dynamics.

According to Eq. (6), the detuning change driven by the derivative feedback tends to counteract any variation of the laser intensity. In fact, when the intensity grows (i.e., $I_n > I_{n-1}$) the system responds, increasing the detuning. This pushes the laser pulse towards the tail of the electron beam distribution causing the gain and, thus, the intensity to decrease [see Eq. (2)]. When $I_n < I_{n-1}$, vice versa: the detuning is reduced, the gain becomes larger, and the intensity tends to grow. Hence, the feedback acts in general against any modulation of the laser intensity, regardless of its intrinsic dynamical origin.

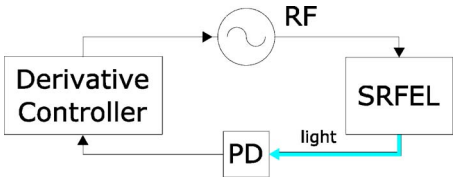

FIG. 9. Schematic layout of the closed-loop derivative feedback: the laser light generated by the SRFEL is acquired by means of a photodiode (PD). The resulting signal is sent to the stabilization system, made of a simple device to obtain the signal derivative, followed by an inverting amplifier with a variable gain. The obtained output is then used to modify the electron-beam revolution period (via the modification of the radio frequency, rf), i.e., the value of the detuning ϵ.

On the basis of the above, one can infer that replacing the detuning ϵ in Eq. (1) with the quantity

$$\epsilon_n = \epsilon_0 + A\,\sin(2\pi f \Delta T n) + \beta(I_n - I_{n-1}), \tag{7}$$

allows one to account, at the same time, for the detuning offset (which may "naturally" drive the system unstable if $\epsilon_0 > \epsilon_c$), the electron-beam instability, and the control of the two previous effects.

A feedback of the type described above has been implemented on the Elettra SRFEL. Results, shown in Figs. 10 and 11 for different initial detuning conditions, confirm the theoretical predictions: the derivative feedback is able to invert the Hopf bifurcation and, at the same time, to counteract the effect of the time-dependent detuning due to the electron-beam instability. The residual oscillations superposed to the almost cw regime are directly related to the limited gain

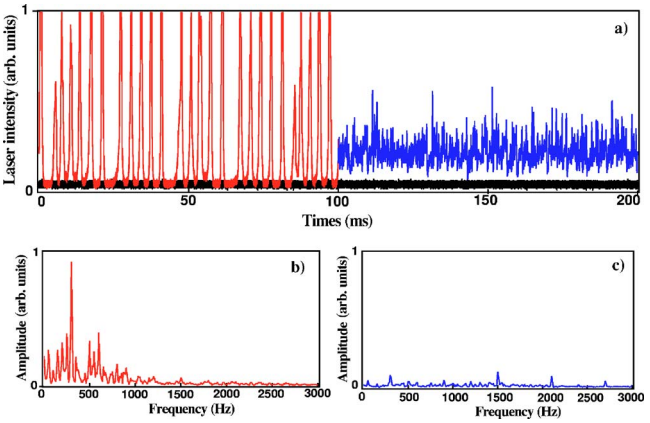

FIG. 10. (a) Temporal behavior of the Elettra FEL intensity without (left part) and with (right part) derivative feedback. (b) Fourier analysis of the signal shown in the left part of (a). (c) Fourier analysis of the signal shown in the right part of (a). FEL operated close to the perfect laser-electron synchronism.

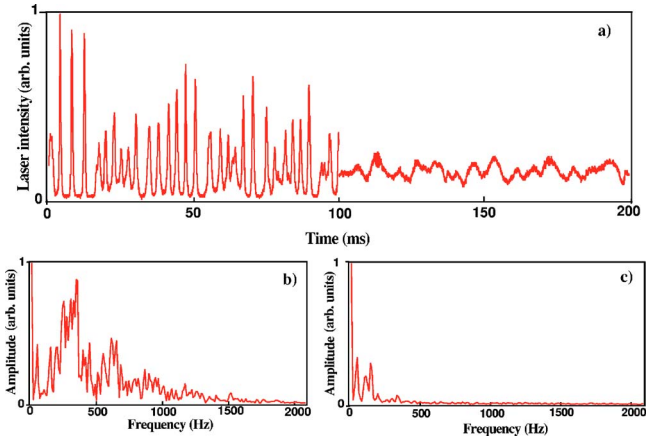

FIG. 11. (a) Temporal behavior of the Elettra FEL intensity without (left part) and with (right part) derivative feedback. (b) Fourier analysis of the signal shown in the left part of (a). (c) Fourier analysis of the signal shown in the right part of (a). FEL operated with a detuning of a few femtoseconds.

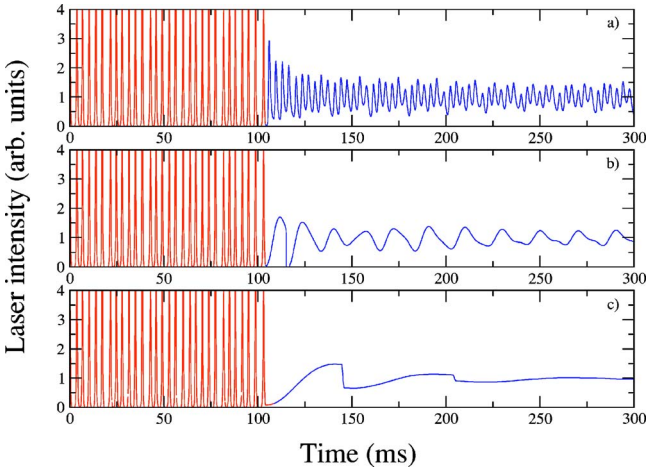

FIG. 12. Numerical behavior of the laser intensity as obtained complementing Eqs. (1)–(3) with (7) (considering a two-frequency modulation). The following parameters have been used: $\epsilon_0 > \epsilon_c$, $A_1 = A_2 = 0.2$ fs, $f_1 = 50$ Hz, $f_2 = 100$ Hz; $\beta = 0$ (left part of the picture) and $\beta = 5 \times 10^{-3}$ (a), $\beta = 3 \times 10^{-1}$ (b), $\beta = 10$ (c) (right part of the picture).

bandwidth of the inverting amplifier. In fact, the gain, related to the factor β in Eq. (7), cannot exceed a given value. Beyond this critical threshold a change in sign for ϵ occurs and the feedback tends to increase the difference between I_n and I_{n+1}, thus amplifying the instability. These considerations suggest a criterion for choosing the initial detuning ϵ_0 so as to optimize the control effectiveness: the offset has to be small enough to maintain the system well inside the detuning curve (see Fig. 2), but, at the same time, so large as to guarantee a wide gain bandwidth. This tradeoff guided the choice of ϵ_0 in the case of Fig. 11, allowing us to attain a better final stability with respect to the (almost zero offset) situation displayed in Fig. 10. A further increase of the feedback gain would have led, in both cases, to the inversion of the detuning sign and, thus, to the instability amplification.

Numerical results obtained by complementing Eqs. (1)–(3) with (7) are in good agreement with experiments. Figures 12(a) and 12(b) refer to different values of β: for β small, as in Fig. 12(a), the induced cw regime remains quite noisy. For larger values of β [see Fig. 12(b)] the fluctuations are strongly reduced. The situation displayed in Fig. 12(b) corresponds, as in the case of Figs. 10 and 11, to the maximum gain before inversion of the detuning sign. In fact, this limitation can, in principle, be overcome by changing the sign of β according to that of the detuning. This would allow a further increase of the feedback gain and, as a consequence, a noticeable improvement of the final stability. Such a strategy has been adopted to get the numerical result shown in Fig. 12(c).

In the aim of testing the robustness of the control technique, the instability perturbing the laser dynamics has been modeled, changing the shape of the modulating function. For instance, square waves with different rise times have been considered. Also in this case, which relates to one of the possible experimental scenarios, the laser intensity may be stabilized by means of a proper choice of the parameter β.

V. CONCLUSIONS AND PERSPECTIVES

The analysis carried out in the first part of this paper allowed us to shed light on the possible mechanisms responsible for the unstable dynamics of the Elettra SRFEL. In particular, within the framework of the theoretical model developed in Refs. [16,17], it was shown that the macrotemporal dynamics of the FEL is highly affected by low-frequency perturbations of the light-electron synchronism. Based on the same model, a control strategy exploiting a closed-loop derivative feedback has been defined in the second part of the paper. The successful implementation of the feedback system made it possible to induce an almost cw regime of the laser intensity.

In order to further improve the FEL stability, we plan to upgrade the feedback system by combining the derivative signal with a signal proportional to the output power. Preliminary results have shown that such a combination may lead to a noticeable reduction of the intensity fluctuations.

ACKNOWLEDGMENTS

We are thankful to the Elettra accelerator group for technical support. We also acknowledge S. Bielawsky, C. Bruni, M. E. Couprie, and G. Lambert for participating in our shifts. The work of G.D.N, B.D., and M.T. has been partially supported by EUFELE, a Project funded by the European Commission under FP5 Contract No. HPRI-CT-2001-50025. This work is part of the PRIN2003 project, "Order and chaos in nonlinear extended systems," funded by MIUR-Italy.

[1] J. L. Laclare, *CERN Report* 85–19, 377 (1985).
[2] A. W. Chao, *Physics of Collective Beam Instabilities in High Energy Accelerators* (Wiley, New York, 1993).
[3] D. Brandt *et al.*, Proceedings EPAC 1992, 345.
[4] D. Bulfone *et al.*, Proceedings EPAC 2002, 2061 (available at http://accelconf.web.cern.ch/accelconf/).
[5] G. De Ninno *et al.*, Proceedings PAC 2003, 2306 (available at http://accelconf.web.cern.ch/accelconf/).
[6] D. Bulfone *et al.*, J. Jpn. Soc. Synchrotron Radiat. Res. **16** (2003).
[7] M. Lonza *et al.*, Proceedings EPAC 2004, 2604 (available at http://accelconf.web.cern.ch/accelconf/).
[8] M. Trovó *et al.*, Proceedings EPAC 2004, 393 (available at http://accelconf.web.cern.ch/accelconf/).
[9] N. A. Vinokurov *et al.*, University of Novossibirsk Report No. INP77-59 (1977).
[10] M. E. Couprie *et al.*, Nucl. Instrum. Methods Phys. Res. A **331**, 37 (1993).
[11] H. Hama *et al.*, Nucl. Instrum. Methods Phys. Res. A **375**, 32 (1996).
[12] M. E. Couprie *et al.*, Nucl. Instrum. Methods Phys. Res. A **475**, 229 (2001).
[13] M. E. Couprie *et al.*, Nucl. Instrum. Methods Phys. Res. A **358**, 374 (1995).
[14] S. Koda *et al.*, Nucl. Instrum. Methods Phys. Res. A **475**, 211 (2001).
[15] G. De Ninno *et al.*, Nucl. Instrum. Methods Phys. Res. A **507**, 274 (2003).
[16] G. De Ninno and D. Fanelli, Phys. Rev. Lett. **92**, 094801 (2004).
[17] G. De Ninno and D. Fanelli Phys. Rev. E **70**, 016503 (2004).
[18] R. P. Walker *et al.*, Nucl. Instrum. Methods Phys. Res. A **429**, 179 (1999).
[19] B. Diviacco *et al.*, Proceedings EPAC 2000, 2322.
[20] A. Gatto *et al.*, Nucl. Instrum. Methods Phys. Res. A **483**, 357 (2002).
[21] M. Trovò *et al.*, Nucl. Instrum. Methods Phys. Res. A **483**, 157 (2002).
[22] G. De Ninno *et al.*, Nucl. Instrum. Methods Phys. Res. A **507**, 274 (2003).
[23] M. E. Couprie *et al.*, Phys. Rev. E **53**, 1871 (1996).
[24] G. De Ninno *et al.*, Nucl. Instrum. Methods Phys. Res. A **483**, 177 (2002).
[25] M. Billardon *et al.*, Phys. Rev. Lett. **69**, 2368 (1992).
[26] G. De Ninno *et al.*, Eur. Phys. J. D **22**, 269 (2003).
[27] C. Bruni, Ph.D. thesis, Université Paris 6, 2000 (unpublished).
[28] S. Bielawski *et al.*, Phys. Rev. A **47**, 3276 (1993).
[29] S. Bielawski *et al.*, Phys. Rev. E **69**, 045502 (2004).
[30] As shown in Fig. 1, an optical klystron [9] consists of two undulators separated by a dispersive section (i.e., a strong magnetic field), whose role is to favor the interference between the emission of the two undulators.